

Depinning exponents of the driven long-range elastic string

Olaf Duemmer* and Werner Krauth†
 CNRS-Laboratoire de Physique Statistique
 Ecole Normale Supérieure
 24 rue Lhomond, 75231 Paris Cedex 05, France

We perform a high-precision calculation of the critical exponents for the long-range elastic string in quenched disorder at the depinning transition, at zero temperature. Large-scale simulations are used to avoid finite-size effects and to enable high precision. The roughness-, growth-, and velocity exponent are calculated independently, and the dynamic- and correlation length exponent are derived from scaling relations. The critical exponents are self-consistent and agree well with analytical predictions.

Driven elastic manifolds in disordered media model a multitude of physical systems ranging from cracks advancing in a solid in response to an external strain field [1] over charge density waves [2], vortices in type-II superconductors in an electric field [3], to magnetic domain walls in an external magnetic field [4]. These widely studied out-of-equilibrium systems undergo dynamic phase transitions [5] as a function of the external driving force (strain, electric or magnetic field, etc). At driving forces below the depinning threshold ($f < f_c$), the disorder pins the manifold so that its asymptotic overall velocity is zero. Above the depinning threshold f_c , avalanches advance the manifold with finite average velocity. At the depinning threshold (for $f \rightarrow f_c^+$) the asymptotic mean velocity goes to zero algebraically, whereas the typical length, width and duration of the avalanches diverge. This critical divergence is characterized by universal scaling exponents.

At the simplest level, advancing crack fronts are modeled by the dynamics of an elastic string driven through quenched disorder (the inhomogeneous material). On that same level, elasticity theory combined with a reasonable energy dissipation mechanism can be reduced to an effective equation of motion for the crack front [1, 6, 7], and the resulting elastic energy kernel is long-range, i.e. falls off as the inverse distance squared. The same long-range elastic energy kernel is found in the wetting problem of an advancing contact line [8].

In the last fifteen years, well-controlled experiments have been designed to measure universal scaling exponents [9, 10, 11, 12]. But the experimental precision available does not yet allow to give definite answers on questions about universality. In addition, experimental results on the roughness exponent of contact lines are inconsistent with theoretical predictions. However, a longstanding controversy on numerical values of the roughness exponent has recently been resolved [13, 14, 15, 16, 17, 18].

In this paper, we perform a numerical simulation of the depinning phase transition of the long-range string driven through quenched disorder, with the aim of computing the critical exponents to high precision. Numerical simulations of this model are in fact non-trivial because of unusually large finite-size effects.

The discrete long-range elastic string is represented by a vector of integer heights $\{h_1, \dots, h_L\}$ with periodic boundary conditions. The string follows discrete quasi-static dynamics while being driven through a discrete disorder (cf. [19]). The long-range elastic force acting on a string element i is given by

$$f_i^{\text{elastic}} = \sum_{j \neq i}^L \frac{h_j - h_i}{|j - i|^2} \quad (1)$$

Even though the sum contains $\sim L$ terms for each of L sites, all forces on all sites can be computed in $\sim L \log L$ operations using a Fast-Fourier-Transform (FFT) algorithm.

The quenched disorder generates a random force η :

$$f_i^{\text{random}} = f + g\eta_i(h_i) \quad (2)$$

While f is a constant external field, the random position-dependent force η is drawn from a binomial distribution: η equals plus one with probability p , and minus one with probability $1 - p$. The coupling g [20] controls the Larkin length at which the elastic and disorder forces balance.

The random force results in a net external driving force of $f + g(2p - 1)$. The parameter f can be adjusted to keep constant the otherwise fluctuating mean velocity v of the string during a simulation. p is the control parameter of the dynamic phase transition: its distance to the critical value p_c (the depinning threshold) controls the large-scale properties of the dynamics, the divergence of the correlation length and the algebraic decay of the mean velocity v [21]. The skewed binomial distribution of random forces corresponds to random-field frozen disorder, as opposed to random bond disorder.

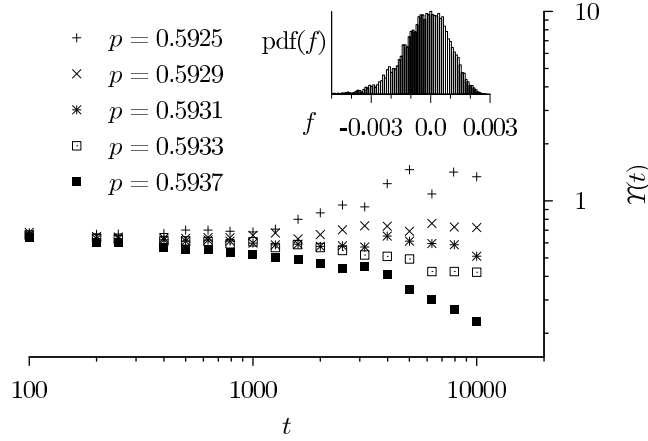


FIG. 1: At the depinning threshold p_c , the ratio $\Upsilon(t) = w/(tv(t))$ is constant in time, as shown by scaling arguments. For $p < p_c$, $\Upsilon(t \rightarrow \infty) \rightarrow \infty$ because the velocity vanishes, and for $p > p_c$, $\Upsilon(t \rightarrow \infty) \rightarrow 0$. The inset shows fluctuations around zero of the external force f for a simulation with fixed p_c and fixed velocity: 0.01 of sites move at each time step.

The microscopic dynamics of the string are given by the following discrete dynamical rule:

$$\Delta h_i(t) = v_i(t) = \begin{cases} 1 & \text{if } f_i^{\text{elastic}} + f_i^{\text{random}} > 0 \\ 0 & \text{otherwise} \end{cases} \quad t = 0, 1, \dots \quad (3)$$

This rule does not allow for backward motion, which is justified by the *no-return* theorem [22]. It states that any initially forward moving string obeying dissipative dynamics and having a convex elastic energy function will never recede in the course of its motion.

The discrete dynamical model can be tuned to the depinning threshold for fixed value of p . It suffices to adjust, at each time step, the parameter f such that a fixed very small fraction of sites advances. In the extreme case, one lets only one site move at a time. This sequential update leads to the smallest possible velocity and tunes the system exactly to the depinning threshold. Used in previous medium size simulations [15, 16], it becomes however too slow for large systems.

Very large system sizes are however crucial in order to calculate the critical exponents with sufficient precision. For example, an accuracy of $\delta\beta = 0.01$ in the velocity exponent requires a resolution of $\delta p_c = 10^{-3}$ in the critical force [23]. This resolution can only be obtained if the finite-sample-size fluctuations of the critical force σ_{p_c} are small enough. From a finite-size-scaling analysis one finds $\sigma_{p_c}(L) = 0.65 \times L^{-1/\nu_{\text{FS}}}$, $\nu_{\text{FS}} = 1.62$ (data not shown), and demanding that $\sigma_{p_c} < 10^{-3}$ gives the minimum system size $L_{\text{min}} \approx 10^5$.

The discretized model, with its coarse and low-cost description of microscopic dynamics, can be simulated for sizes up to $L = 2^{20} \approx 10^6$, more than three orders of magnitude larger than earlier discrete [15, 16] and continuum simulations [24].

To translate the high speed of the FFT algorithm into a fast simulation, we use parallel updating. The elastic force for all string elements is calculated and the dynamic rule (equation 3) is applied simultaneously to all sites. Then the random force is updated for those sites that have stepped forward. In this way a single vector of length L suffices to store the random force, avoiding storage problems even for very large system sizes. The parallel updating leads to a fluctuating mean velocity v , whereas the external driving force is kept constant via the fixed control parameter p .

In the simulations with fluctuating mean velocity, the depinning threshold p_c is determined by adapting a technique known from absorbing-state dynamic phase transitions [25]. We start the simulation for fixed p , $f = 0$ from a flat line at $t = 0$, and monitor the ratio of string width $w(t) \equiv \text{Var}(h_i(t))^{1/2}$ to decaying mean velocity $v(t) \equiv \langle v_i(t) \rangle$ times time t :

$$\text{At threshold : } v(t) \sim \frac{w(t)}{t} = t^{\zeta/z-1}, \quad \implies \Upsilon(t) \equiv \frac{w(t)}{tv(t)} \sim \text{const.}$$

To understand why the velocity at threshold is given by the width divided by time, we remark that, intuitively, an avalanche takes time t to advance a distance equal to its width $w(t)$. And at threshold the complete motion of the string is solely due to avalanches, hence the mean velocity is given by $v(t) = w(t)/t$. It follows that the ratio $\Upsilon(t)$

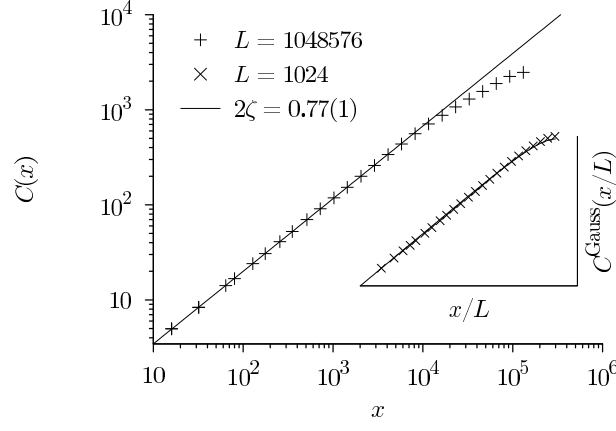


FIG. 2: *Roughness exponent* ζ . At short distances, the two-point correlation function scales as $C(x) \propto x^{2\zeta}$. A linear fit gives $\zeta = 0.385(5)$ (Average is taken over pinned configurations exactly at $p = p_c$). The inset compares correlation function data (for $L = 1024$) with the Gaussian model of eq. 4.

is constant at threshold. Away from threshold it either grows to infinity (for $p < p_c$) or decays to zero (for $p > p_c$), providing a very sensitive indicator for the depinning threshold.

The main plot in figure 1 illustrates how $\Upsilon(t)$ is very sensitive to changes in $p - p_c$, which in turn enables a very precise localization of the critical threshold $p_c = 0.5931(2)$. p_c can alternatively be extracted from a power-law fit of the steady-state mean velocity ($v \sim (p - p_c)^\beta$, see figure 5).

We emphasize the equivalence between on the one hand a dynamical simulation at fixed driving force and fluctuating velocity, and on the other hand the self-organizing dynamics at fixed-velocity and fluctuating driving force. We use fixed driving force dynamics throughout this paper, but as a check, we performed a fixed velocity simulation by adjusting the parameter f at each time step such that exactly 0.01 of all sites move [26]. With fixed very small velocity $v = 0.01$ and fixed value of $p = p_c$ we monitor the fluctuations in f . The inset of figure 1 shows that f fluctuates around a mean value of zero, demonstrating that we are indeed at the critical point $p = p_c$.

The roughness exponent $\zeta = 0.388$ [18] characterizes the self-affine spatial structure of the string at depinning, and the scaling properties of its average width $w = \langle (h_i - \bar{h})^2 \rangle^{1/2}$ (see also [27]). As a check for the discrete model, we compute this exponent from the short-distance behavior of the two-point correlation function $C(x) \equiv \langle (h(0) - h(x))^2 \rangle \sim x^{2\zeta}$. Averaging over pinned configurations exactly at the depinning threshold $p = p_c$, we confirm earlier results ($\zeta = 0.385(5)$, see figure 2).

The correlation function $C(x)$ can be fitted over the whole interval $x \in [0, 0.5L]$ using the Gaussian model [28]: Suppose the random string configuration $h(x)$ is decomposed into Fourier modes

$$h(x) = \sum a_n \cos(2\pi nx/L) + b_n \sin(2\pi nx/L),$$

where a_n and b_n are Gaussian random variables with variance $\sigma_n^2 \propto 1/n^{1+2\zeta}$. The resulting two-point correlation function is given by $C^{\text{Gauss}}(x) = 4 \sum_n \sin^2[\pi nx/L] / n^{2\zeta+1}$, with the following expansion for small x/L [28] (note the difference between the roughness exponent ζ and the Riemann zeta-function ζ_R):

$$C^{\text{Gauss}}(x) = \text{const} \left\{ - \left(\frac{x}{L} \right)^{2\zeta} 2^{-1+2\zeta} \pi^{2\zeta} \Gamma(-2\zeta) \sin \frac{\pi(2\zeta+1)}{2} + \left(\frac{x}{L} \right)^2 \frac{2\pi^2}{2!} \zeta_R(2\zeta-1) - \left(\frac{x}{L} \right)^4 \frac{8\pi^4}{4!} \zeta_R(2\zeta-3) + O \left[\left(\frac{x}{L} \right)^6 \right] \right\} \quad (4)$$

This function is used in the inset of figure 2 to fit the correlation function data obtained with the exact algorithm [29] for smaller systems. The fit remains excellent even for large x/L .

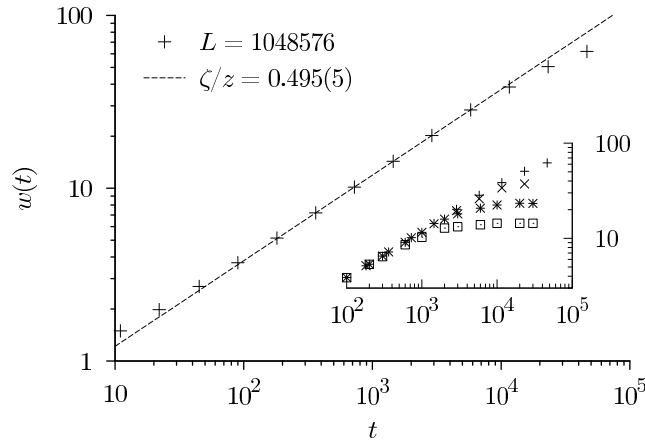


FIG. 3: *Growth exponent ζ/z .* The algebraic growth of the average width $w(t)$, at the depinning threshold ($p = p_c$) and after an initial decay of discretization effects ($t \sim 100$), gives the growth exponent $\zeta/z = 0.495(5)$. Inset: large finite-size effects as width levels off at $w_L \sim L^\zeta$, $L = \{2^{14}, \dots, 2^{20}\}$.

The dynamic exponent z was previously estimated in discrete extremal models of limited size [15, 16]. We determine it via the growth exponent ζ/z , which controls the growth of the average width with time $w(t) \sim t^{\zeta/z}$. This algebraic growth law results from the two scaling laws for the width and the time in terms of the correlation length ξ : $w \sim \xi^\zeta$ and $\xi \sim t^{1/z}$. Starting at $t = 0$ from a flat line, at the critical point $p = p_c$, and monitoring the growth of the average width, we find (see figure 3) the growth exponent to be $\zeta/z = 0.495(5)$, implying $z = 0.770(5)$ for the dynamic exponent. The width $w(t)$ is also affected by large finite-size effects. The algebraic growth regime is limited by the width of the entire string $w_L \sim L^\zeta$. The inset of figure 3 demonstrates how $w(t)$ saturates at the system-size-dependent limit w_L . The plots for different system sizes L can be superposed by plotting $w(t)L^{-\zeta}$ versus tL^{-z} .

Another way of determining the dynamic exponent z is to analyze the time-dependent structure factor $S(q, t) \equiv \langle h(q, t)h(-q, t) \rangle$ with the Fourier transform of the height given by $h(q) \equiv \sum_{n=0}^{L-1} \exp(iqn)h_n$ and $q \equiv 2\pi k/L$, where $k \in \{0, \dots, L-1\}$ is the mode-number. The structure factor allows to illustrate both the dynamic growth of the interface and its self-affine structure in space-time [30]:

$$S(q, t) \sim q^{-1-2\zeta} \Phi(q^z t) \quad \text{with} \quad \Phi(y) = \begin{cases} y^{\frac{1+2\zeta}{z}}, & y \rightarrow 0 \\ \text{const}, & y \rightarrow \infty \end{cases} \quad (5)$$

Figure 4 illustrates how the different Fourier modes $S(q, t)$ converge to their steady-state value $\sim q^{-1-2\zeta}$ after a relaxation time q^{-z} . The small-time behavior $S(q, t) \sim t^{(1+2\zeta)/z}$ provides the dynamic exponent, and we confirm the numerical value $z = 0.77(1)$, albeit with lower precision than in the analysis using $w(t)$. The inset of figure 4 gives a plot of $S(q, t)q^{1+2\zeta}$ versus the dimensionless quantity $q^z t$, showing the universal scaling form Φ , and demonstrating how the dynamic exponent z links time t and (inverse) space q in a self-affine way.

The velocity exponent β controls the power-law decrease of the mean velocity with the distance to the critical threshold: $v \sim (p - p_c)^\beta$. It is obtained from the averaged center-of-mass velocity $v \equiv \frac{1}{L} \sum_i v_i$ in the steady state regime (see figure 5). From a fit at fixed p_c , we obtain $\beta = 0.625(5)$. The data of the steady-state velocity can also be fitted to obtain the threshold p_c , as shown in the inset of figure 5. Only for $p = p_c$ is there a straight line on the log-log plot. For $p \neq p_c$, a clear non-zero curvature emerges.

Note that it is quite difficult to obtain a precise estimate for β , again because of large finite-size effects. Trying to calculate β on medium size systems one faces the problem of a significantly reduced critical scaling regime. It manifests itself already in the short-range elastic model [24], and is even more pronounced on long-range elastic interfaces of intermediate size (data not shown). Again one needs to go to very large system sizes in order to obtain sufficient accuracy.

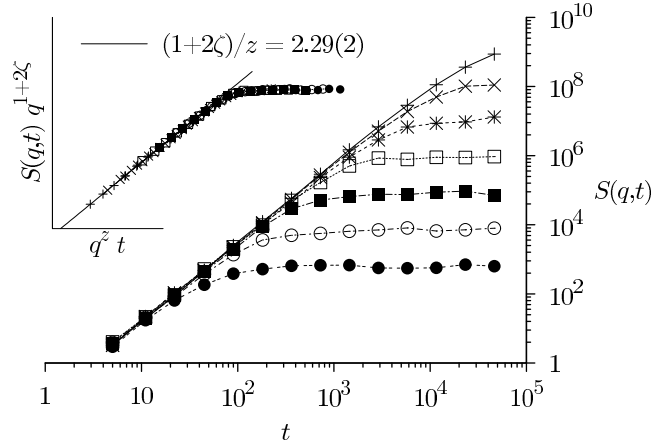


FIG. 4: *Time-dependent structure factor* $S(q,t)$. Different Fourier components [from (+) $q = 3 \times 10^{-6}$ to (\bullet) $q = 10^{-2}$] take a relaxation time of q^{-z} to reach their steady-state value of $q^{-1-2\zeta}$. Inset: The small-time behavior of the universal scaling function gives a further estimate of the dynamic exponent $z = 0.77(1)$.

The value obtained for the velocity exponent yields an independent calculation of the growth exponent ζ/z , via two scaling relations that reduce the set of four critical exponents to two independent ones: the statistical tilt symmetry [31] links the roughness exponent to the correlation length exponent $\nu = 1/(1 - \zeta)$, and a further scaling relation links all four exponents $\beta = \nu(z - \zeta)$ [31]. Using these two equalities and values of $\zeta = 0.385(5)$ and $\beta = 0.625(5)$ one confirms the roughness exponent to be $\zeta/z = 0.495(5)$, or equivalently the dynamic exponent $z = 0.770(5)$. The correlation length exponent finally is given by $\nu = 1.625(10)$.

In conclusion, we have numerically solved the non-equilibrium depinning phase transition of the long-range elastic string driven through quenched disorder. The values obtained for the critical exponents are self-consistent and agree with analytical predictions [13, 14]. It will be interesting to understand why exactly the roughness and growth exponents calculated in this paper agree with those measured in a recent crack front experiment [32], whether they can also be seen in wetting experiments, and more generally, if universality can be confirmed as the physical mechanism unifying these diverse phenomena.

We thank D. Bonamy, E. Bouchaud, H. Chaté, A. Colton, P. Le Doussal, S. Guibert, L. Ponson, A. Rosso, and K. J. Wiese for stimulating discussions.

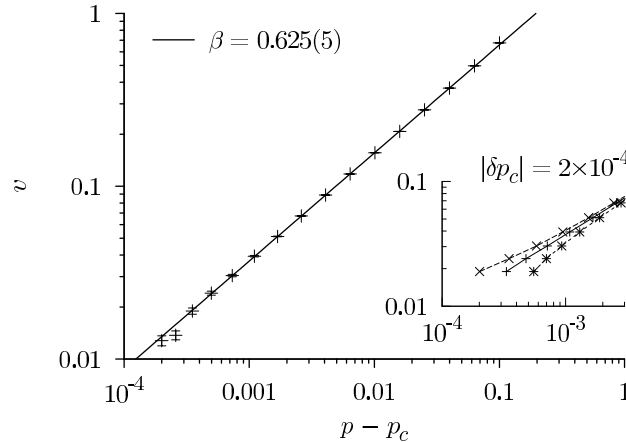


FIG. 5: *Velocity exponent* β . The steady-state mean velocity for different values of $p - p_c$ gives the velocity exponent: $\beta = 0.625(5)$. Inset: slightly wrong values of p_c lead to non-zero curvature [(\times) $p_c \rightarrow p_c - \delta p_c$, (\ast) $p_c \rightarrow p_c + \delta p_c$].

* Electronic address: duemmer@lps.ens.fr

† Electronic address: krauth@lps.ens.fr

- [1] H. Gao, J. R. Rice, *J. Appl. Mech.* **56**, 828 (1989).
- [2] G. Grüner, *Rev. Mod. Phys.* **60**, 1129 (1988).
- [3] G. Blatter *et al.* *Rev. Mod. Phys.* **66**, 1125 (1994).
- [4] S. Lemerle *et al.* *Phys. Rev. Lett.* **80**, 849 (1998).
- [5] D. S. Fisher, *Phys. Rev. B* **31**, 1396 (1985).
- [6] S. Ramanathan, D. Ertas, D. S. Fisher, *Phys. Rev. Lett.* **79**, 873 (1996).
- [7] J. P. Bouchaud, E. Bouchaud, G. Lapasset, J. Planès, *Phys. Rev. Lett.* **71**, 2240 (1993).
- [8] J. F. Joanny, P. G. De Gennes, *J. Chem. Phys.* **81**, 552 (1984).
- [9] K. L. Måløy, S. Santucci, J. Schmittbuhl, R. Toussaint, *Phys. Rev. Lett.* **96**, 045501 (2006).
- [10] S. Moulinet, C. Guthmann, E. Rolley, *Eur. Phys. J. E*, **8**, 437 (2002).
- [11] A. Prevost, E. Rolley, C. Guthmann, *Phys. Rev. B*, **65**, 064517 (2002).
- [12] L. Ponson, D. Bonamy, E. Bouchaud, *Phys. Rev. Lett.* **93**, 035506 (2006).
- [13] O. Narayan, D. S. Fisher, *Phys. Rev. B*, **48**, 7030 (1993).
- [14] P. Chauve, P. Le Doussal, K. J. Wiese, *Phys. Rev. Lett.* **86**, 1785 (2001); P. Le Doussal, K. J. Wiese, P. Chauve, *Phys. Rev. B*, **66**, 174201 (2002).
- [15] J. Schmittbuhl, S. Roux, J. P. Vilotte, K. J. Maloy, *Phys. Rev. Lett.* **74**, 1787 (1995).
- [16] A. Tanguy, M. Gounelle, S. Roux *Phys. Rev. E*, **58**, 1577 (1998).
- [17] S. Ramanathan, D. S. Fisher, *Phys. Rev. B*, **58**, 6026 (1998).
- [18] A. Rosso, W. Krauth, *Phys. Rev. E*, **65**, 025101(R) (2005).
- [19] H. Leschhorn, T. Nattermann, S. Stepanow, L. H. Tang, *Ann. Physik*, **6**, 1 (1997).
- [20] We set $g = 1$ throughout this paper.
- [21] Peculiarly, setting $p = 1/2$ while letting f approach the critical value $f_c = g(2p_c - 1)$ is not equivalent to our procedure. The discreteness of the model entails in this case that the asymptotic velocity does not approach zero continuously as $f \rightarrow f_c$, it rather drops discontinuously from a value of order unity at $f > f_c$ to zero at $f \leq f_c$.
- [22] A. A. Middleton, *Phys. Rev. Lett.* **68**, 670 (1992).
- [23] Taking differentials of $v \sim (p - p_c)^\beta$ implies $\delta\beta/\beta = -\delta p_c/(|p - p_c| \log |p - p_c|)$ and measuring the β -slope at $p - p_c \approx 0.01$ in figure 5 gives $\delta p_c \approx 10^{-3}$.
- [24] O. Duemmer, W. Krauth *Phys. Rev. E*, **71**, 061601 (2005).
- [25] H. Hinrichsen, *Adv. Phys.* **49**, 815-958 (2000).
- [26] We choose $v = 0.01$ because this is the limit of statistical resolution of a system of size $L \approx 10^6$ (cf. figure 5), and furthermore a sequential update of a single site is too time consuming since we would have to recalculate all elastic forces ($\sim L \log L$) each time a single site advances.
- [27] D. Vandembroucq, S. Roux, *Phys. Rev. E*, **70**, 026103 (2004).
- [28] A. Rosso, R. Santachiara, W. Krauth, *J. Stat. Mech. Theory E*, L08001 (2005); R. Santachiara, A. Rosso, W. Krauth, cond-mat/0611326.
- [29] A. Rosso, W. Krauth, *Phys. Rev. B*, **65**, 012202 (2001).
- [30] A. L. Barabási, H. E. Stanley *Fractal Concepts in Surface Growth* CUP, Cambridge (1995).
- [31] T. Nattermann, S. Stepanow, L. H. Tang, H. Leschhorn, *J. Phys. (France)* **II 2**, 1438 (1992).
- [32] D. Bonamy, L. Ponson, S. Prades, E. Bouchaud, C. Guillot, *Phys. Rev. Lett.* **97**, 135504 (2006).